Extension of the exact trajectory model to the case of asymmetric tops and its application to infrared nitrogen-broadened linewidths of ethylene

Jeanna Buldyreva*
Institut UTINAM, UMR CNRS 6213, Université de Franche-Comté, 16 route de Gray, 25030 Besançon cedex, France

Linh Nguyen
Laboratoire Lasers et Spectroscopies, Facultés Universitaires Notre-Dame de la Paix, 61 rue de Bruxelles, B-5000 Namur, Belgium
(Received 6 December 2007; revised manuscript received 21 March 2008; published 24 April 2008)

The model of exact trajectories involved in a semiclassical computation of (vib)rotational linewidths and shifts is extended to the case of asymmetric top colliders. General expressions for the second-order contributions to the scattering matrix are given which define the pressure broadening and shift of the line. This theoretical approach is tested on the particular case of the infrared ν_7 band linewidths of C_2H_4 broadened by N_2 which is frequently required for atmospheric applications. The computed linewidths compare favorably with available experimental data.

DOI: 10.1103/PhysRevA.77.042720 PACS number(s): 34.10.+x, 33.70.Jg

I. INTRODUCTION

Asymmetric top molecules such as H_2O, O_3, or C_2H_4 assume an important place in the physical chemistry of the Earth's and planetary atmospheres. Their remote sensing by spectroscopic techniques enables a study of complex processes such as ozone layer depletion or greenhouse effect. Due to low molecular symmetry, from the experimental point of view, the spectra of these species recorded in the infrared and microwave regions appear as dense manifolds of (vib)rotational lines hardly accessible for accurate and exhaustive measurements while, from the theoretical point of view, the interaction potential energy surfaces are not precisely known and quantum-mechanical approaches are not applicable. Up to now, the most advanced computations of asymmetric-top spectral parameters are provided by semiclassical methods which combine the quantum-mechanical description of the internal molecular degrees of freedom (vibrations and rotations) with a simplified, classical, treatment of the relative molecular motion (translations). For the water molecule semiclassical computations have been made [1–4] in the framework of the original approach of Robert and Bonamy (RB) [5] which improves the well-known Anderson-Tsao-Curnutte (ATC) theory [6,7] by avoiding the unphysical cutoff procedure for the scattering operator via the linked cluster theorem [8,9], curved parabolic trajectories governed by the isotropic part of the intermolecular potential, and taking into account the short-range interactions. In other works [10–12] the fully complex implementation of the RB formalism (CRB) proposed by Gamache *et al.* [13] has been used. The ozone case has been considered by Hartmann *et al.* [14] as well as by Bouazza *et al.* [15] within the RB approach of Refs. [1–3] and also by Gamache and co-workers (see, e.g., Refs. [16,17]) with the CRB formulation. Semiclassical RB computations for ethylene have been made in Refs. [18–22] but treating this molecule as linear. All the abovementioned authors studying asymmetric rotors obtained quite realistic theoretical values though some molecular parameters such as the quadrupolar moment for C_2H_4 [20] or atom-atom interaction parameters for O_3-N_2 and O_3-O_2 systems [15] were sometimes kept free in order to get the best fit to the available experimental data. In any case, additional detailed input information on the intermolecular potential, (vib)rotational wave functions and energy levels was needed from independent sources making computations much more heavy and tedious than for linear or symmetric top rotors. Another difficulty of semiclassical computation for polyatomic [23,24] (and diatomic [25]) molecules consists in the fact that these methods are not free from some approximations necessary for rototranslational decoupling and may lose their precision for highly anisotropic colliders with strong short-range interactions. The interpretation of semiclassical calculation results for asymmetric tops represents thus a quite delicate problem since a possible disagreement with experimental values can arise from both imprecise input parameters and computational method itself.

A possible further improvement of semiclassical approaches lies in the trajectory model used for computations. Instead of straight-line trajectories of the ATC theory or parabolic trajectories of the original RB approach, Bykov *et al.* [26,27] proposed to directly employ the exact solutions of the classical equations of motion for a particle in an isotropic potential field [28] but did not compute linewidth. This exact trajectory model was introduced in the RB formalism for the line broadening of linear molecules in Ref [29]; later, an extension was made to symmetric tops [30]. For all molecular systems considered, the new model based on exact trajectories provided much more realistic theoretical values than any previous approach using straight-line or parabolic trajectories. We present in this paper a generalization of the RB formalism with exact trajectories (RBE) to the case of asymmetric tops completing and finalizing thus the series of our previous works on this subject.

The theory is applied to the ethylene molecule C_2H_4 since it is a nearly prolate symmetric top allowing a comparison with the simplified "prolate top" consideration of Refs. [18,22]. Moreover, it is one of important pollutants of the

*jeanna.buldyreva@univ-fcomte.fr

terrestrial atmosphere produced by industrial processes, automobile traffic, vegetation, forest fires (the latter are, for example, detectable from the space owing to C_2H_4 presence [31]). It is also created by photodissociation of methane in the stratosphere of Titan [32] and outer planets [33,34] and constitutes an important probe molecule for their atmosphere investigation. The single frequency region relatively well studied for this purpose lies between 800 and 1500 cm^{-1} (tetrad $\nu_{10}/\nu_7/\nu_4/\nu_{12}$) [35] and is therefore worthy of being investigated by our theoretical approach. The choice of nitrogen as perturber is due to the atmospheric needs as well as to quite exhaustive information available in the literature on its molecular parameters and existing line shape computations for C_2H_4-N_2 system [18,22].

The paper is organized as follows. The next section outlines the key points of the RB formalism with exact trajectories and details its extension to the asymmetric top colliders. Particular attention is paid to the expansion of the intermolecular potential on the rotational invariants and to the representation of the rotational wave functions. Section III contains an application of the theoretical approach to the case of ethylene infrared lines broadened by nitrogen at room temperature. The molecular and spectroscopic features of the ethylene molecule are recalled for completeness. The behavior of computed linewidths as a function of various quantum and pseudoquantum numbers is analyzed and compared with a number of available experimental data as well as with other existing theoretical estimates. The concluding remarks and some perspectives of application are summarized in the final section.

II. THEORETICAL CONSIDERATIONS

A. RB formalism with exact trajectories

The basic expression of the original RB formalism [5] gives the half-width on the half of height (HWHH) γ_{fi} of a (vib)rotational spectral line corresponding to the radiative transition $f \leftarrow i$ (in cm^{-1}) as

$$\gamma_{fi} = \frac{n_b}{2\pi c}\sum_{J_2}\rho_{J_2}\int_0^\infty vf(v)dv\int_0^\infty 2\pi b db \times\left[1-(1-S^{(L)}_{2,f2i2})e^{\left[-(S_{2,f2}+S_{2,i2}+S^{(C)}_{2,f2i2})\right]}\right] \quad (1)$$

(inelastic vibrational contributions and noncommutativity of the interaction potential in the interaction representation are neglected). In this equation n_b is the number density of perturbing particles and ρ_{J_2} is their thermal population in the (ground-state) rotation levels J_2. Instead of the averaging with the Maxwell-Boltzmann distribution of velocities $f(v)$, the mean thermal velocity $\bar{v}=\sqrt{8k_BT/(\pi m^\star)}$ (k_B is the Boltzmann constant, T is the temperature, and $m^\star$ is the reduced mass of the molecular pair) is commonly used in order to minimize the CPU time without a noticeable loss of precision. Furthermore, the integration over the impact parameter b can be rewritten as the integration over the distance of the closest approach r_c which are related via the energy and momentum conservation condition $b/r_c=[1-V^\star_{\rm iso}(r_c)]^{1/2}$, where $V^\star_{\rm iso}$ denotes the reduced value of the isotropic part of the interaction potential $V_{\rm iso}$ defined by $V^\star_{\rm iso}=2V_{\rm iso}/(m^\star v^2)$. The second-order contributions to the scattering matrix are given by the matrix elements of the anisotropic part $V_{\rm aniso}$ in the basis of molecular system wave functions integrated over the collision duration [5]

$$S_{2,i2}=\frac{\hbar^{-2}}{2(2J_i+1)(2J_2+1)}\sum_{\substack{\{i'\}J_i'M_i'\{2'\}J_2'M_2'\\ M_iM_2}}\left|\int_{-\infty}^{\infty}dt e^{i\omega_{\{i\}J_i\{2\}J_2,\{i'\}J_i'\{2'\}J_2't}}\langle\{i\}J_iM_i\{2\}J_2M_2|V_{\rm aniso}[\vec{r}(t)]|\{i'\}J_i'M_i'\{2'\}J_2'M_2'\rangle\right|^2, \quad (2)$$

$$S^{(C)}_{2,f2i2}=\sum_{J_2'}S_{2,f2'i2'}\delta_{J_2'J_2},\quad S^{(L)}_{2,f2i2}=\sum_{J_2'\neq J_2}S_{2,f2'i2'}, \quad (3)$$

where

$$S_{2,f2'i2'}=-\frac{\hbar^{-2}}{(2J_i+1)(2J_2+1)}\sum_{\substack{M_iM_i'M_fM_f'\\ M_2M_2'M}}C^{J_iM_i}_{J_fM_f\rho\sigma}C^{J_iM_i'}_{J_fM_f'\rho\sigma}\int_{-\infty}^{\infty}dt e^{i\omega_{\{2'\}J_2'\{2\}J_2t}}\langle\{f\}J_fM_f'\{2'\}J_2'M_2'|V_{\rm aniso}[\vec{r}(t)]|\{f\}J_fM_f\{2\}J_2M_2\rangle$$
$$\times\int_{-\infty}^{\infty}dt' e^{i\omega_{\{2\}J_2\{2'\}J_2't'}}\langle\{i\}J_iM_i\{2\}J_2M_2|V_{\rm aniso}[\vec{r}(t')]|\{i\}J_iM_i'\{2'\}J_2'M_2'\rangle. \quad (4)$$

In Eqs. (2)–(4) the primes mark the values after collision and $\{i\}$ ($\{f\}$) and $\{2\}$ in the wave functions stand for other than rotational and magnetic quantum numbers of the active molecule in the initial (final) state and of the perturbing molecule, respectively. The $S_{2,f2}$ contribution for the final state is given simply by changing i into f in Eq. (2). The frequency denoted by $\omega_{\{i\}J_i\{2\}J_2,\{i'\}J_i'\{2'\}J_2'}$ in Eq. (2) is the sum of two frequencies $\omega_{\{i\}J_i,\{i'\}J_i'}$ and $\omega_{\{2\}J_2,\{2'\}J_2'}$ of the transitions induced by collision in the active and perturbing molecules.

The Clebsch-Gordan coefficients $C^{J_iM_i}_{J_fM_f\rho\sigma}$ and $C^{J_iM_i'}_{J_fM_f'\rho\sigma}$ in Eq. (4) describe the coupling between the active molecule and the external field (tensorial order $\rho=0$ for the isotropic Raman scattering, $\rho=1$ for the electric dipolar absorption and $\rho=2$ for the anisotropic Raman scattering).

The computation of the second-order contributions by Eqs. (2)–(4) requires a specification of the trajectory model (integrals over time) as well as the interaction potential and the wave functions (matrix elements). Since the relative translational motion is decoupled from molecular vibrations and rotations, the time dependence of V_{aniso} is completely contained in the intermolecular distance vector $\vec{r}$. The latter is governed by V_{iso} and describes a plane trajectory whose radial $r(t)$ and angular $\Psi(t)$ parts are defined by the trajectory model chosen. The integration over time t in Eqs. (2) and (4) can be therefore replaced by the integration over the intermolecular distance r. When the parabolic trajectory, a Lennard-Jones form of the isotropic potential as well as an analytical model for V_{aniso} are employed in the framework of the traditional RB formalism, the S_2 terms appear as analytical functions of molecular parameters; moreover, the variable change in the integral over b in Eq. (1) is straightforward:

$$bdb = r_c dr_c \left(\frac{v_c'}{v}\right)^2 \tag{5}$$

(v_c' is the apparent velocity defined by v, r_c and Lennard-Jones parameters) [5]. The model of exact trajectories gives t and Ψ as functions of r [28]:

$$t = \int_{r_c}^{r} \frac{dr'}{\sqrt{2[\mathcal{E} - V_{\text{iso}}(r')]/m^\star - \mathcal{M}^2/(m^{\star 2} r'^2)}} + c_1, \tag{6}$$

$$\Psi = \int_{r_c}^{r} \frac{\mathcal{M}/r'^2 dr'}{\sqrt{2m^\star[\mathcal{E} - V_{\text{iso}}(r')] - \mathcal{M}^2/r'^2}} + c_2, \tag{7}$$

where $\mathcal{E}=m^\star v^2/2$ and $\mathcal{M}=m^\star bv$ are, respectively, the energy and angular momentum of the colliding pair. The integration constants c_1 and c_2 vanish if the collision takes place in the plane XOY, so that at $t=0$, $r=r_c$, and $\Psi=0$. This model is not limited to a preselected mathematical form of the isotropic potential and evaluates the time integrals in Eqs. (2) and (4) by a numerical integration over r through

$$dt = dr/\sqrt{2[\mathcal{E} - V_{\text{iso}}(r)]/m^\star - \mathcal{M}^2/(m^{\star 2} r^2)} \tag{8}$$

(the second-order contributions cannot anymore be written analytically). The corresponding integration over the impact parameter is performed using the relation [36]

$$bdb = r_c dr_c \left[1 - V^\star_{\text{iso}}(r_c) - \frac{r_c}{2} V^{\star\prime}_{\text{iso}}(r_c)\right], \tag{9}$$

where a numerical differentiation of $V^\star_{\text{iso}}$ (denoted by the prime) is needed.

In the framework of semiclassical approaches the molecular wave functions are proper to the internal molecular degrees of freedom and are consequently not affected by the trajectory model. For pure rotational motion of linear molecules they are given by ordinary spherical harmonics tied to the orientation of the molecular axis in the laboratory-fixed frame

$$|JM\rangle = Y_{JM}(\theta,\phi) \tag{10}$$

(J is the quantum number for the total angular momentum $\vec{J}$ and M is its projection on the laboratory Z axis). For symmetric rotors they are proportional to the rotational D-matrices (Wigner matrices) [37]:

$$|JKM\rangle = \left(\frac{2J+1}{8\pi^2}\right)^{1/2} D^J_{-K,-M}(\chi,\theta,\phi), \tag{11}$$

where the additional quantum number K stands for the projection of $\vec{J}$ on the molecular z axis (χ axis) and (ϕ,θ,χ) are the Euler angles of the principal-axes molecular system relative to the space-fixed laboratory axes. We underline that the rotational matrix in this equation contains the arguments ϕ and χ in reversed order and can be related to the corresponding D matrix with usual order by [38]

$$D^J_{KM}(\chi,\theta,\phi) = (-1)^{K-M} D^J_{MK}(\phi,\theta,\chi). \tag{12}$$

When using the exact trajectories, the expansion of the interaction potential has to be made in the laboratory-fixed frame. For linear molecules this potential is easily written as a simple series of spherical harmonics tied to the orientations of both molecular axes $[Y_{l_1m_1}(\Omega_1)$ and $Y_{l_2m_2}(\Omega_2)]$ and of the intermolecular distance vector $\vec{r}$ $[Y_{lm}(\Omega)]$ [25,39,40]:

$$V(\vec{r}) = \sum_{l_1l_2l} V_{l_1l_2l}(r) \sum_{m_1m_2m} C^{lm}_{l_1m_1l_2m_2} \times Y_{l_1m_1}(\Omega_1) Y_{l_2m_2}(\Omega_2) Y_{lm}(\Omega)^*. \tag{13}$$

Here Ω_x denotes the polar angles of the molecule x ($x=1,2$) while Ω stands for the polar angles of $\vec{r}$ and the asterisk means the complex conjugation. For colliders of arbitrary symmetry two first spherical harmonics are replaced by rotational Wigner matrices [25,39,40]

$$V(\vec{r}) = \sum_{l_1l_2l} \sum_{k_1k_2} V^{k_1k_2}_{l_1l_2l}(r) \sum_{m_1m_2m} C^{lm}_{l_1m_1l_2m_2} \times D^{l_1}_{m_1k_1}(\Omega_1)^* D^{l_2}_{m_2k_2}(\Omega_2)^* Y_{lm}(\Omega)^*, \tag{14}$$

where the arguments Ω_x correspond now to the complete sets of Euler angles ϕ_x,θ_x,χ_x. [Another rotationally invariant expansion of $V(\vec{r})$ into series of D matrices with reversed arguments can be found in Ref. [38].]

B. Case of asymmetric rotors

A molecule having three different principal moments of inertia is an asymmetric top. These moments of inertia I_a, I_b, and I_c tied, respectively, to the rotations about a, b, and c axes ($I_a<I_b<I_c$) determine the corresponding rotational constants A, B, C ($A>B>C$) [41]. The asymmetry is char-

acterized by the coefficient $\kappa=(2B-A-C)/(A-C)$ which takes values between -1 and $+1$. The low-limit value $\kappa=-1$ corresponds to the prolate symmetric top $(B=C)$, the high-limit value $\kappa=1$ refers to the oblate symmetric top $(A=B)$ and $\kappa=0$ gives the most asymmetric top.

The qualitative picture of the asymmetric top energy levels represents consequently an intermediate case between the energy level manifolds of prolate and oblate symmetric tops. (Appropriate diagrams for the correlation of the asymmetric top energy levels with those of prolate and oblate symmetric tops can be found, for instance, in Refs. [41,42].) In the asymmetric top each value of rotational quantum number J gives rise to $2J+1$ different energy levels (due to the removal of the double degeneracy on quantum number K when passing from the symmetric to the asymmetric top). There is, however, no meaningful quantum number to distinguish these $2J+1$ energy levels. They are simply labeled by an index τ varying from $-J$ to J as the energy increases. At the same time, each J_τ level, starting from the zeroth one, may be sequentially and univocally connected to one prolate-top level (J,K_{-1}) and one oblate-top level (J,K_1) [41,42] so that instead of τ the pair of indices K_{-1} and K_1 can be used. Since for the prolate top the quantum number K corresponds to the projection on the least-moment-of-inertia axis a, K_{-1} is often called K_a in the literature. For the oblate symmetric top K means the projection on the largest-moment-of-inertia axis c and the notation K_c is used instead of K_1 . The indices K_{-1},K_1 (or K_a,K_c) characterizing the asymmetric tops are sometimes referred to as "pseudoquantum" numbers since they are good quantum numbers only in the limit of prolate and oblate symmetric tops. Both indices vary from 0 to J but while K_{-1} increases with increasing energy levels, K_1 varies in the opposite direction. The energy levels of the asymmetric top cannot be represented by explicit formulae, and approximate expressions or a numerical solution for the eigenvalues of the rotational Hamiltonian are employed. The numerical solution is possible since for any asymmetric top molecule the Hamiltonian matrix tied to a particular J value is split into four submatrices corresponding to four irreducible representations of the group D_2 with the basic functions given in Table V of Ref. [38].

The rotational wave functions of the asymmetric top commonly denoted by $|J\tau M\rangle$ may be expressed in terms of symmetric top wave functions $|JKM\rangle$ as [38]

$$|J\tau M\rangle = \sum_K a_K^{J\tau}|JKM\rangle, \tag{15}$$

where the coefficients $a_K^{J\tau}$ depend on the chosen form of the rotational Hamiltonian and are obtained simultaneously with the rotational energies during a numerical diagonalization procedure. The calculation of matrix elements with the rotational functions of asymmetric top reduces therefore to the evaluation of the same operator in the basis of symmetric top wave functions using the relation [38]

$$\langle JKM|D_{km}^l|J'K'M'\rangle = \sqrt{\frac{2J'+1}{2J+1}}C_{J'K'l-k}^{JK}C_{J'M'l-m}^{JM}. \tag{16}$$

The interaction potential for two asymmetric rotors, contrary to the case of linear molecules, depends not only on the orientations of the molecular axis of each partner in the laboratory frame but also on the rotation of each molecule about this axis (radial components depend additionally on the projections k_1, k_2). The computations with exact trajectories use therefore the potential expansion on spherical harmonics introduced in Eq. (14).

C. Interaction potential for asymmetric tops

In order to specify the radial components $V_{l_1l_2l}^{k_1k_2}(r)$ a potential model has to be chosen. Since for polyatomic molecules there is, in general, no numerical potential computed by quantum-mechanical methods, we adopt here the commonly used atom-atom model for the short-range forces to which the long-range electrostatic interactions are added:

$$V = V^{aa} + V^{\mathrm{el}}. \tag{17}$$

For molecules of arbitrary symmetry, including the asymmetric top ones, the potential energy of the long-range electrostatic interactions (for which $l=l_1+l_2$) can be expressed in terms of spherical harmonics [40]

$$V^{\mathrm{el}}(\vec{r}) = \sum_{l_1l_2l}\sum_{k_1k_2} A_{l_1l_2}\frac{Q_{l_1k_1}Q_{l_2k_2}}{r^{l+1}}\delta_{l,l_1+l_2}\sum_{m_1m_2m} C_{l_1m_1l_2m_2}^{lm} \times D_{m_1k_1}^{l_1}(\Omega_1)^* D_{m_2k_2}^{l_2}(\Omega_2)^* Y_{lm}(\Omega)^*, \tag{18}$$

where $Q_{l_xk_x}$ represent the spherical multipole components in the molecular frame and the coefficients $A_{l_1l_2}$ are given by

$$A_{l_1l_2} = \frac{(-1)^{l_2}}{2l+1}\left[\frac{(4\pi)^3(2l+1)!}{(2l_1+1)!\,(2l_2+1)!}\right]^{1/2}. \tag{19}$$

The potential energy of atom-atom interactions approximated by Lennard-Jones dependences reads [43]

$$V^{aa} = \sum_{i,j}\left(\frac{d_{ij}}{r_{1i,2j}^{12}} - \frac{e_{ij}}{r_{1i,2j}^{6}}\right), \tag{20}$$

where d_{ij} and e_{ij} are the atomic pair energy parameters and $r_{1i,2j}$ is the distance between the ith atom of the first molecule and the jth atom of the second molecule. In order to put Eq. (20) into the form of Eq. (14) the two-center expansion of the function $r_{1i,2j}^{-n}$ (in the nonoverlapping region $r > r_{1i}+r_{2j}$) has to be made [44,45]:

$$r_{1i,2j}^{-n} = \sum_{l_1l_2l} f_{l_1l_2l}^n(r_{1i},r_{2j},r)\sum_{m_1m_2m} C_{l_1m_1l_2m_2}^{lm} \times Y_{l_1m_1}(\Omega_{1i})Y_{l_2m_2}(\Omega_{2j})Y_{lm}(\Omega)^* \tag{21}$$

with

$$f^n_{l_1 l_2 l}(r_{1i}, r_{2j}, r) \equiv \frac{(-1)^{l_2}}{r^n}\left[\frac{(4\pi)^3(2l_1+1)(2l_2+1)}{(2l+1)}\right]^{1/2} C^{l0}_{l_1 0 l_2 0} \times \sum_{p,q}\left(\frac{r_{1i}}{r}\right)^p\left(\frac{r_{2j}}{r}\right)^q \frac{(n+p+q-l-3)!!\,(n+p+q+l-2)!!}{(n-2)!\,(p-l_1)!!\,(p+l_1+1)!!\,(q-l_2)!!\,(q+l_2+1)!!}[1+\delta_{n1}(\delta_{pl_1}\delta_{ql_2}\delta_{p+q,l}-1)], \tag{22}$$

$p=l_1, l_1+2, l_1+4, \ldots$, and $q=l_2, l_2+2, l_2+4, \ldots$. In Eq. (21) Ω_{1i} and Ω_{2j} represent the orientations of $\vec{r}_{1i}$ and $\vec{r}_{2j}$ vectors in the laboratory-fixed frame. Since for polyatomic molecules the atoms i,j may be located out of the molecular axes described by Ω_1 and Ω_2 [see Eq. (14)], the spherical harmonics $Y_{l_1 m_1}(\Omega_{1i})$ and $Y_{l_2 m_2}(\Omega_{2j})$ must be rewritten as functions of Ω_1 and Ω_2 [40]:

$$Y_{l_x m_x}(\Omega_{xi}) = \sum_{k_x} D^{l_x}_{m_x k_x}(\Omega_x)^* Y_{l_x k_x}(\Omega'_{xi}), \tag{23}$$

where Ω'_{xi} is the orientation of the ith atom of the xth molecule in the molecular frame.

The final expression for the radial components of the full interaction potential in form of Eq. (14) is given therefore by

$$V^{k_1 k_2}_{l_1 l_2 l}(r) = A_{l_1 l_2}\frac{Q_{l_1 k_1} Q_{l_2 k_2}}{r^{l+1}}\delta_{l,l_1+l_2} + \sum_{ij}[d_{ij} f^{12}_{l_1 l_2 l}(r_{1i}, r_{2j}, r) - e_{ij} f^{6}_{l_1 l_2 l}(r_{1i}, r_{2j}, r)] Y_{l_1 k_1}(\Omega'_{1i}) Y_{l_2 k_2}(\Omega'_{2j}). \tag{24}$$

Since the exact trajectory approach involves a numerical integration of the radial potential components $V^{k_1 k_2}_{l_1 l_2 l}(r)$ over r, these components are also computed numerically. In addition, this numerical computation enables a test of convergence with respect to p and q parameters of the two-center expansion.

D. Calculation of second-order contributions for asymmetric tops

The general form of Eq. (14) for the interaction potential leads to the matrix elements

$$\langle J_i \tau_i M_i J_2 \tau_2 M_2 | V_{\text{aniso}}[\vec{r}(t)] | J'_i \tau'_i M'_i J'_2 \tau'_2 M'_2 \rangle = \sum_{l_1 l_2 l}\sum_{k_1 k_2} V^{k_1 k_2}_{l_1 l_2 l}[r(t)] \sum_{m_1 m_2 m} C^{lm}_{l_1 m_1 l_2 m_2} Y_{lm}[\Omega(t)]^* \times \langle J_i \tau_i M_i | D^{l_1}_{m_1 k_1}(\Omega_1)^* | J'_i \tau'_i M'_i \rangle \langle J_2 \tau_2 M_2 | D^{l_2}_{m_2 k_2}(\Omega_2)^* | J'_2 \tau'_2 M'_2 \rangle, \tag{25}$$

where

$$\langle J_i \tau_i M_i | D^{l_1}_{m_1 k_1}(\Omega_1)^* | J'_i \tau'_i M'_i \rangle = \sqrt{\frac{2J'_i+1}{2J_i+1}} \sum_{K_i K'_i} a^{J_i \tau_i *}_{K_i} a^{J'_i \tau'_i}_{K'_i} C^{J_i K_i}_{J'_i K'_i l_1 k_1} C^{J_i M_i}_{J'_i M'_i l_1 m_1}, \tag{26}$$

and

$$\langle J_2 \tau_2 M_2 | D^{l_2}_{m_2 k_2}(\Omega_2)^* | J'_2 \tau'_2 M'_2 \rangle = \sqrt{\frac{2J'_2+1}{2J_2+1}} \sum_{K_2 K'_2} a^{J_2 \tau_2 *}_{K_2} a^{J'_2 \tau'_2}_{K'_2} C^{J_2 K_2}_{J'_2 K'_2 l_2 k_2} C^{J_2 M_2}_{J'_2 M'_2 l_2 m_2}, \tag{27}$$

in accordance with Eqs. (15) and (16).

Introducing the notations

$$X^{l_1}_{k_1}(J_i \tau_i J'_i \tau'_i) \equiv \sum_{K_i K'_i} a^{J_i \tau_i *}_{K_i} a^{J'_i \tau'_i}_{K'_i} C^{J'_i K'_i}_{J_i K_i l_1 k_1}, \quad X^{l_2}_{k_2}(J_2 \tau_2 J'_2 \tau'_2) \equiv \sum_{K_2 K'_2} a^{J_2 \tau_2 *}_{K_2} a^{J'_2 \tau'_2}_{K'_2} C^{J'_2 K'_2}_{J_2 K_2 l_2 k_2}, \tag{28}$$

and

$$I^{k_1 k_2}_{l_1 l_2 l m}(\omega) \equiv \int_{-\infty}^{\infty} dt e^{i\omega t} V^{k_1 k_2}_{l_1 l_2 l}[r(t)] Y_{lm}[\Omega(t)]^* \tag{29}$$

we can write the $S_{2,i2}$ term of Eq. (2) and $S_{2,f2'i2'}$ term of Eq. (4) as

$$S_{2,i2} = \frac{1}{2\hbar^2}\sum_{J'_i \tau'_i J'_2 \tau'_2}\sum_{l_1 l_2 l}\frac{1}{(2l_1+1)(2l_2+1)}\sum_m \left|\sum_{k_1 k_2}(-1)^{k_1+k_2} X^{l_1}_{-k_1}(J_i \tau_i J'_i \tau'_i) X^{l_2}_{-k_2}(J_2 \tau_2 J'_2 \tau'_2) I^{k_1 k_2}_{l_1 l_2 l m}(\omega_{i2,i'2'})\right|^2, \tag{30}$$

$$S_{2,f2'i2'} = -\frac{(-1)^{J_i+J_f+J_2+J_2'+\rho}}{\hbar^2}\sqrt{\frac{(2J_2'+1)(2J_i+1)(2J_f+1)}{(2J_2+1)}}\sum_{l_1l_2l}\frac{(-1)^{l_2+l}W(J_iJ_fJ_iJ_f;\rho l_1)}{(2l_1+1)(2l_2+1)}$$
$$\times\sum_m\left[\sum_{k_1k_2}(-1)^{k_1+k_2}X^{l_1}_{-k_1}(J_f\tau_fJ_f\tau_f)X^{l_2}_{-k_2}(J_2'\tau_2'J_2\tau_2)I^{k_1k_2}_{l_1l_2lm}(\omega_{2'2})\right]$$
$$\times\left[\sum_{\eta_1\eta_2}(-1)^{\eta_1+\eta_2}X^{l_1}_{-\eta_1}(J_i\tau_iJ_i\tau_i)X^{l_2}_{-\eta_2}(J_2\tau_2J_2'\tau_2')I^{k_1k_2}_{l_1l_2lm}(\omega_{22'})\right] \quad (31)$$

where $W(J_iJ_fJ_iJ_f;\rho l_1)$ is a Racah coefficient.

The integral of Eq. (29) can be further simplified using the trajectory symmetry and the properties of the spherical harmonics

$$Y_{lm}(\theta,\phi)^* = [(2l+1)(l-m)!/(4\pi)/(l+m)!]^{1/2}$$
$$\times e^{-im\phi}P_l^m(\cos\theta)$$

[46] for the chosen orientation of the laboratory frame (the collision takes place in the plane XOY so that $\Omega=(\pi/2,\Psi)$ and the associated Legendre polynomials

$$P_l^m(0) = (-1)^{(l+m)/2}(l+m)!/[(l-m)/2]!/[(l+m)/2]!$$

do not vanish only when $l+m$ is even):

$$I^{k_1k_2}_{l_1l_2lm}(\omega) = 2\frac{(-1)^{(l+m)/2}\sqrt{(l-m)!\,(l+m)!}}{2^l[(l-m)/2]!\,[(l+m)/2]!}$$
$$\times\int_0^\infty dt\,\cos[\omega t - m\Psi(t)]\tilde{V}^{k_1k_2}_{l_1l_2l}[r(t)], \quad (32)$$

where the radial potential components $\tilde{V}^{k_1k_2}_{l_1l_2l}=[(2l+1)/(4\pi)]^{1/2}V^{k_1k_2}_{l_1l_2l}$. Replacing further the integration over t by the integration over r with the exact trajectory formulas (6)–(8) and introducing the dimensionless integration variable $y=r/r_c$ give

$$I^{k_1k_2}_{l_1l_2lm}(\omega) = \frac{2r_c}{v}\frac{(-1)^{(l+m)/2}\sqrt{(l-m)!\,(l+m)!}}{2^l[(l-m)/2]!\,[(l+m)/2]!}\tilde{I}^{k_1k_2}_{l_1l_2lm}(\omega), \quad (33)$$

where

$$\tilde{I}^{k_1k_2}_{l_1l_2lm}(\omega) \equiv \int_1^\infty \frac{dyy\tilde{V}^{k_1k_2}_{l_1l_2l}(yr_c)\cos[k_cA_0(y) - m\sqrt{1-V^\star_{\rm iso}(r_c)}A_2(y)]}{\sqrt{y^2-1+V^\star_{\rm iso}(r_c)-y^2V^\star_{\rm iso}(yr_c)}}, \quad (34)$$

$$A_n(y) = \int_1^y \frac{dz}{z^{n-1}\sqrt{z^2-1+V^\star_{\rm iso}(r_c)-z^2V^\star_{\rm iso}(zr_c)}}, \quad (35)$$

and $k_c=\omega r_c/v$ is the resonance parameter. To compute the terms S_2 further, a precise specification of the interacting molecules is needed.

III. APPLICATION TO C_2H_4-N_2

For a linear perturbing molecule (N_2) $k_2=K_2=K_2'=0$ so that the corresponding $X^{l_2}_0$ function is equal to $C^{J_2'0}_{J_20l_20}$ and the second-order contributions reduce to

$$S_{2,i2} = \frac{2r_c^2}{\hbar^2v^2}\sum_{J_i'\tau_i'J_2'}\sum_{l_1l_2l}\frac{(C^{J_2'0}_{J_20l_20})^2}{(2l_1+1)(2l_2+1)}\sum_m\frac{(l-m)!\,(l+m)!}{2^{2l}[(l-m)/2]!^2[(l+m)/2]!^2}\left|\sum_{k_1}(-1)^{k_1}X^{l_1}_{-k_1}(J_i\tau_iJ_i'\tau_i')\tilde{I}^{k_10}_{l_1l_2lm}(\omega_{i2,i'2'})\right|^2, \quad (36)$$

$$S_{2,f2'i2'} = -\frac{4r_c^2(-1)^{J_i+J_f+J_2+J_2'+\rho}}{\hbar^2v^2}\sqrt{(2J_i+1)(2J_f+1)}\sum_{l_1l_2l}\frac{(-1)^lW(J_iJ_fJ_iJ_f;\rho l_1)}{(2l_1+1)(2l_2+1)}(C^{J_2'0}_{J_20l_20})^2\sum_m\frac{(l-m)!\,(l+m)!}{2^{2l}[(l-m)/2]!^2[(l+m)/2]!^2}$$
$$\times\left[\sum_{k_1}(-1)^{k_1}X^{l_1}_{-k_1}(J_f\tau_fJ_f\tau_f)\tilde{I}^{k_10}_{l_1l_2lm}(\omega_{2'2})\right]\left[\sum_{\eta_1}(-1)^{\eta_1}X^{l_1}_{-\eta_1}(J_i\tau_iJ_i\tau_i)\tilde{I}^{\eta_10}_{l_1l_2lm}(\omega_{22'})\right]. \quad (37)$$

For the long-range part of the interaction potential we retained only the principle quadrupole-quadrupole contribution with the spherical nonvanishing components in the principle-axes molecular frame [40]

$$Q_{20} = \sqrt{\frac{5}{4\pi}}Q_{zz}, \quad Q_{22} = Q_{2,-2} = \sqrt{\frac{5}{24\pi}}(Q_{xx}-Q_{yy}). \quad (38)$$

The Cartesian components Q_{xx}, Q_{yy}, Q_{zz} corresponding to the molecular frame presented in Fig. 1 are listed in Table I.

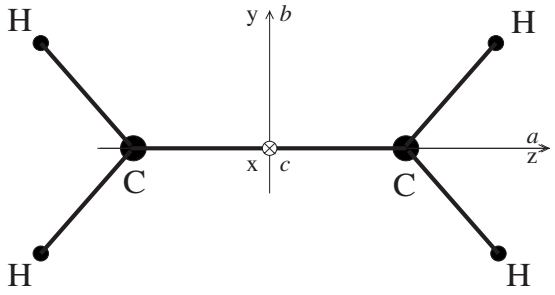

FIG. 1. Geometry of C_2H_4.

For the atom-atom contributions we included the $V_{l_1 l_2 l}^{k_1 k_2}$ terms with $l_1 l_2 l = 022$, 202, 220, 222, and 224; the necessary molecular parameters are also given in Table I. It is worthy of note that among the data of this table the quadrupole moment components are quite well known whereas the pair atom-atom parameters are calculated by the usual combination rules from the homonuclear atom-atom parameters optimized in Ref. [47] by fitting of second virial coefficients to their experimental values. These atom-atom parameters have an important impact on the linewidth computation since in addition to the contribution to the anisotropic part of the intermolecular potential they define its isotropic part which governs the relative trajectory. The energy levels and the coefficients of the C_2H_4 wave functions expansion following Eq. (15) are taken from Ref. [48]. The (ground-state $v=0$) rotational constant value $B_0^{N_2}=1.989622$ [22] is used to compute the rotational energies of the perturbing molecule N_2. The integration over exact trajectories is performed with the mean thermal velocity (which excludes the orbiting collisions) as in the original RB approach [5].

The plane molecule C_2H_4 is a nearly prolate top ($\kappa = -0.9143$ in the ground state). It belongs to the point group D_{2h} and possesses therefore twelve normal vibration modes. For our theoretical analysis we retained the well studied experimentally ν_7 band ($\kappa=-0.9149$ [18]) corresponding to the symmetry type B_{1u}. According to the active molecule geometry (Fig. 1) the normal vibration ν_7 gives rise to a dipolar moment μ_c along the principle symmetry axis c. For the quantum number J we have thus the usual selection rule for radiative transitions in asymmetric tops

$$\Delta J = 0, \pm 1 \tag{39}$$

(Q, R, and P branches, respectively) completed by the selection rule for the alternating dipole moment lying in the axis of the largest moment of inertia

TABLE I. Molecular parameters for C_2H_4-N_2 system.

d_{ij} [a] 10^{-7} erg Å^{12}	e_{ij} [a] 10^{-10} erg Å^6	$\lvert r_{xi}\rvert$ [b] Å	Q [c] 10^{-26} esu
$d_{CN}=0.3230$	$e_{CN}=0.2920$	$\lvert r_{1C}\rvert=0.6765$	$Q_{xx}^{C_2H_4}=-3.25$
$d_{HN}=0.0570$	$e_{HN}=0.0803$	$\lvert r_{1H}\rvert=1.5265$	$Q_{yy}^{C_2H_4}=1.62$
		$\widehat{HCH}=119°55'$	$Q_{zz}^{C_2H_4}=1.63$
		$\lvert r_{2N}\rvert=0.550$	$Q_{zz}^{N_2}=-1.4$

[a]Computed with data of Ref. [47].
[b]Reference [41] for C_2H_4 and Ref. [22] for N_2.
[c]Reference [40].

TABLE II. Selection rules for K_a, K_c indices of C_2H_4 for the radiative transitions of ν_7 band.

ΔJ	$J+\tau$	$\Delta K_a+\Delta K_c$	ΔK_a, ΔK_c included in computation
1	even/odd	1	$\Delta K_a=1$, $\Delta K_c=0$
			$\Delta K_a=-1$, $\Delta K_c=2$
0	even	1	$\Delta K_a=1$, $\Delta K_c=0$
			$\Delta K_a=-1$, $\Delta K_c=2$
	odd	−1	$\Delta K_a=-1$, $\Delta K_c=0$
			$\Delta K_a=1$, $\Delta K_c=-2$
−1	even/odd	−1	$\Delta K_a=-1$, $\Delta K_c=0$
			$\Delta K_a=1$, $\Delta K_c=-2$

$$++ \leftrightarrow +-; -+ \leftrightarrow --\tag{40}$$

which refers to the symmetry of the rotational eigenfunction [41]. The allowed changes of the pseudoquantum numbers K_a, K_c follow the particular rules for μ_c [42]:

$$\Delta K_a = \pm 1, \pm 3, \pm 5, \ldots; \Delta K_c = 0, \pm 2, \pm 4, \ldots \tag{41}$$

which are additionally limited by the allowed changes of K_a+K_c for each ΔJ value and for $J+\tau$ even or odd (see Table II). The collision-induced transitions in the active molecule are determined by the Clebsch-Gordan coefficient $C_{J_i K_i l_1 k_1}^{J_i' K_i'}$ which imposes $J_i - l_1 < J_i' < J_i + l_1$ and $K_i' = K_i + k_1$. For our computations, similar to Refs. [18,22], we accounted generally only for $\Delta K_a = 0$ since including other cases made the computations too time consuming. For the linear and centrosymmetric perturbing molecule l_2 takes only even values ($l_2 = 0, 2, 4, \ldots$) and nonvanishing Clebsch-Gordan coefficients $C_{J_2' 0 l_2 0}^{J_2' 0}$ appear for $J_2' + J_2$ even, so that the collisional transitions in the perturbing molecule occur with $J_2' = J_2 - l_2, J_2 - l_2 + 2, \ldots, J_2, \ldots, J_2 + l_2 - 2, J_2 + l_2$.

We studied first (Fig. 2) the general J dependence of the Q-branch linewidths [four transitions of the $^PQ(J,1)$ sub-branch, one transition of the $^PQ(J,3)$ sub-branch, and one transition of the $^PQ(J,4)$ sub-branch; for all $\Delta K_c = 0$] with the single electrostatic quadrupole-quadrupole contribution with a double goal: to verify the statement of Ref. [22] that the electrostatic contributions alone lead to results underestimated by up to 70% and to test the role of collision-induced transitions with $\Delta K_a \neq 0$ neglected in this reference. As can be seen from this figure, the electrostatic contribution computed as in Ref. [22] with $\Delta K_a = 0$ only (open circles) does give the linewidths underestimated by about 70–80 %. When the corresponding atom-atom contributions are added (filled circles) this discrepancy decreases to 10–20 % showing thus the extreme importance of these particular atom-atom terms. Taking then into account the other possible ΔK_a values (solid squares) yields a further improvement of the computed linewidths which now either coincide completely with the measurements or differ by about 5% only; we must conclude thus that the collisional transitions with $\Delta K_a \neq 0$

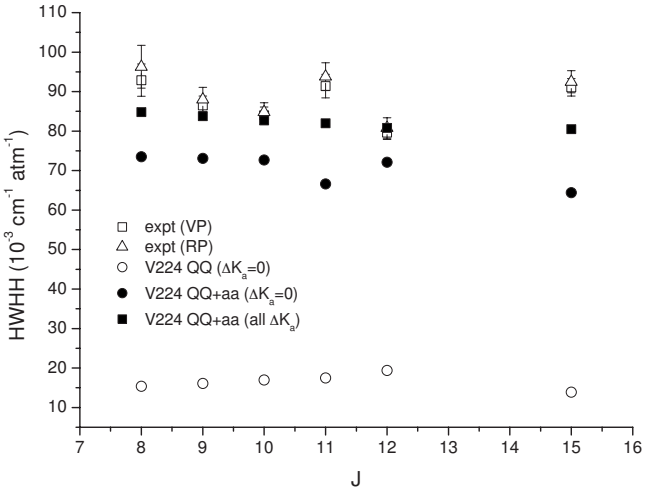

FIG. 2. Study of electrostatic and atom-atom 224 contributions with various selection rules for collisional transitions; experimental values from Ref. [22] are shown for Voigt profile model (VP) and Rautian profile model (RP).

have an observable impact on the line broadening computation. (In further computations we were obliged, however, to limit the collisional transitions to $\Delta K_a=0$ because of the too high CPU cost.)

In order to be sure of the linewidth convergence with respect to l_1, l_2, l values accounted for in our computation we carried out additional tests whose results for the transitions with $\Delta J=0$, $\Delta K_a=-1$, $\Delta K_c=0$ ($3_{13}\rightarrow 3_{03}$, $4_{14}\rightarrow 4_{04}$, …) are presented in Fig. 3. Starting from 224 contributions (both electrostatic and atom-atom: filled circles), we added progressively the atom-atom contributions 222 (solid triangles), 220 (solid diamonds), 202 (crosses), and 022 (solid squares). We can see, for example, that the contribution 202 appears to be quite significant in the line broadening, as it must be for the interaction of the quite anisotropic C_2H_4 molecule with the almost isotropic molecule N_2. At the same time, the "isotropic part" of C_2H_4 ($l_1=0$) and the "anisotropic $l_2=2$ part" of N_2 are not expected to interact strongly, and we can observe in the figure that, indeed, the last contribution $l_1=0$, $l_2=2$ gives almost negligible changing in the linewidth value.

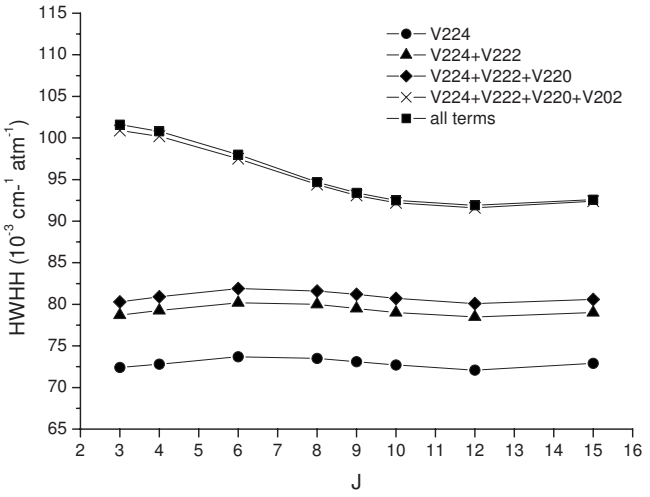

FIG. 3. Test of linewidth convergence for the accounted values of $l_1 l_2 l$ in the interaction potential.

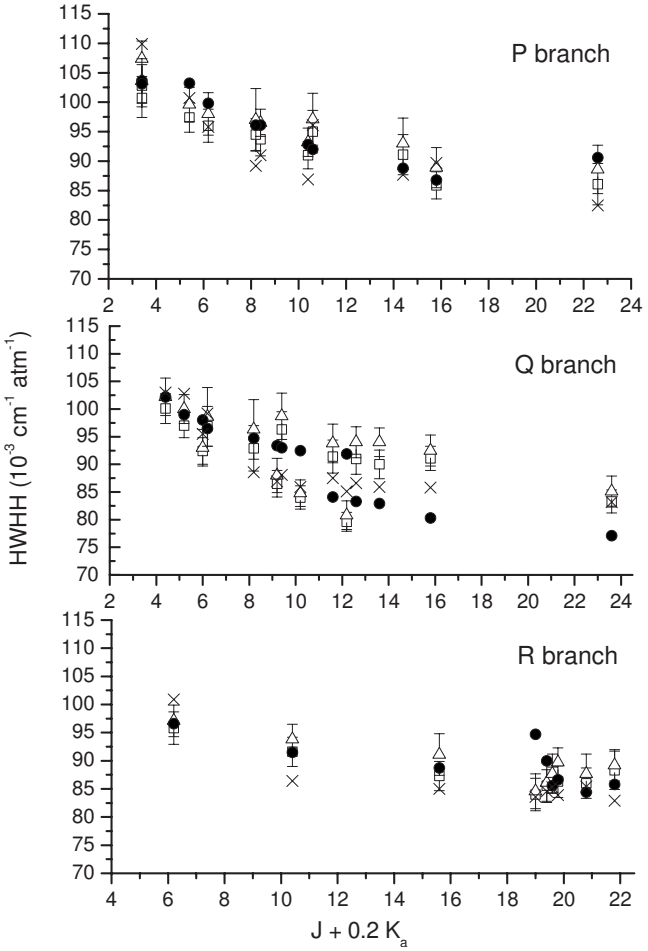

FIG. 4. Linewidth dependence on the rotational quantum number for P, Q, and R branches. Experimental results of Refs. [18,22]: □, Voigt profile, △, Rautian profile. Theoretical results: ×, traditional RB approach [22], ●, RBE approach (this work).

The general J dependence of the line broadening coefficients in the P, Q, and R branches is shown in Fig. 4. For the rotational quantum numbers with few K_a observed experimentally (for instance, $J=19$ in the R branch has $K_a=0,2,3,4$) the detailed analysis of these dependences is hard to be made because of a strong overlapping of the corresponding symbols. In order to resolve this problem, we have chosen a specific representation, with the abscissa incremented by $0.2K_a$. The factor of 0.2 was chosen since for any considered transition $K_a\leq 4$ and all linewidths referring to the same J value have their abscissae between J and $J+0.8$, without interference with the abscissa interval for the next value of the rotational quantum number $J+1$. The RBE-computed linewidths are plotted together with the experimental and theoretical RB values of Refs. [18,22]. In the P branch, in comparison with the traditional RB estimation of linewidths [22], clearly better results are obtained for middle J values. In the Q branch, our computed values are closer to the experimental data for some J values but are, however, more distant for other ones. In the R branch, the agreement of our theoretical values with measurements is almost perfect

(except for $J=19$) whereas the linewidths obtained by the traditional RB approach [22] are clearly overestimated or underestimated. This latter branch allows us to equally look at the K_a dependences of the line broadening coefficients since for $J=19$ three transitions are experimentally available for the sub-branch ${}^{R}R(19,K_a)$ with $K_a=0,2,3$ and $\Delta K_c=0$. For this particular J value, however, our theoretical values are not satisfactory for $K_a=0,2$ and the experimentally observed (with large error bars) linewidth increasing with K_a increasing is not reproduced; it is, however, well predicted by the traditional RB approach of Ref. [22]. At the same time, the theoretical linewidth of this reference for the transition $20_{3,17} \leftarrow 19_{4,15}$ is almost out of the experimental error bar whereas our approach yields a value exactly corresponding to the measurement with a Voigt profile.

The overall comparison with experimental values of P and R branches is therefore more favorable for RBE linewidths (one point for P branch and two points for the R branch outside the experimental error bars instead of respectively five and three points for the RB values). In addition, since the interaction potential is almost identical in both works (the 70% underestimation of linewidths retrieved in our computation with the quadrupole-quadrupole contributions only testifies the negligible role of the higher-order multipole terms included in the interaction potential of Ref. [22]), our better values for the linewidths prove the importance of the correct treatment of C_2H_4 molecule as asymmetric top and the advantage of the exact trajectory model.

The discrepancies still observed between our theoretical results and experimental values can be attributed, from the one hand, to the approximate character of the available interaction potential: a precise theoretical approach needs a refined potential whereas a rough theoretical model can mask the potential imperfections. More reliable atom-atom parameters could improve therefore our theoretical predictions. (For the high J values of the Q branch the neglected because of CPU cost collisional transitions with $\Delta K_a \neq 0$ are possibly also important.) From the other hand, the polyatomic active molecule C_2H_4 is quite anisotropic, so that the decoupling of its rotational and translational motions becomes questionable at small values of the intermolecular distance. Since the model of exact trajectories brings a more precise, with respect to parabolic or straight-line trajectories, description of this region, the nonvalidity of the rototranslational decoupling can induce worse values of the line broadening parameters. For a really pertinent comparison of RB and RBE approaches in the case of asymmetric tops, the active molecule, from one side, must be quite isotropic and interact with the perturber principally by the long-range forces (in order that the rototranslational decoupling be valid) and, from the other side, must have observable short-range contributions in the interaction potential (in order that the short-range difference between the trajectory models can be tested). It seems, however, difficult to satisfy both requirements simultaneously for real molecular pairs.

IV. CONCLUSION

In the present work we have generalized the semiclassical approach of Robert and Bonamy with exact trajectories to the case of asymmetric top molecules. The second-order contributions to the scattering matrix which define the line broadening and shift coefficients are expressed as functions of the radial anisotropic potential components integrated over exact isotropic trajectories and weighted by the coefficients of the asymmetric-top wave function expansion over the wave functions of symmetric top. In comparison with the traditional RB formalism for asymmetric tops, our RBE approach deals with arbitrary (numerical) form of the interaction potential, which allows an easy test of the radial potential components convergence with respect to the parameters of two-center expansion (e.g., the CRB formalism is limited to the eighth order) and avoids the errors induced by fitting of the isotropic potential to analytical Lennard-Jones dependences. Formally, it yields the most precise trajectory description possible in the semiclassical framework. The general formulas are detailed for the particular case of the asymmetric-top C_2H_4 molecule colliding with the centrosymmetric linear molecule N_2 which is of great importance for atmospheric applications.

Comparison of the computed linewidths with the available experimental data and the theoretical values found from a simplified treatment of C_2H_4 as a prolate top in the framework of the traditional parabolic-trajectory RB approach has revealed the importance of the exact asymmetric-top treatment of this molecule, the non-negligible character of collisional transitions with $\Delta K_a \neq 0$ as well as a general improvement of the line broadening prediction with exact classical trajectories. The scarce experimental data have not allowed to draw a definite conclusion on the K_a dependences of the linewidths which appear to be quite different for the two theoretical approaches considered. New measurements are therefore needed to address this point. Other perturbing molecules are also worthy of study.

[1] B. Labani, J. Bonamy, D. Robert, J. M. Hartmann, and J. Taine, J. Chem. Phys. **84**, 4256 (1986).
[2] J. M. Hartmann, J. Taine, J. Bonamy, B. Labani, and D. Robert, J. Chem. Phys. **86**, 144 (1987).
[3] B. Labani, J. Bonamy, D. Robert, and J. M. Hartmann, J. Chem. Phys. **87**, 2781 (1987).
[4] A. Bauer, M. Gordon, J. Carlier, and R. R. Gamache, J. Mol. Spectrosc. **176**, 45 (1996).
[5] D. Robert and J. Bonamy, J. Phys. (Paris) **40**, 923 (1979).
[6] P. W. Anderson, Phys. Rev. **76**, 647 (1949).
[7] C. J. Tsao and B. Curnutte, J. Quant. Spectrosc. Radiat. Transf. **2**, 44 (1961).
[8] R. Kubo, *Fluctuation, Relaxation and Resonance in Magnetic Systems* (ter Haar, Oliver and Boyd, London, 1962).
[9] C. Bloch, Nucl. Phys. **7**, 451 (1958).
[10] R. R. Gamache, R. Lynch, and L. R. Brown, J. Quant. Spec-

trosc. Radiat. Transf. **56**, 471 (1996).
[11] R. R. Gamache, R. Lynch, J. J. Plateaux, and A. Barbe, J. Quant. Spectrosc. Radiat. Transf. **57**, 485 (1997).
[12] R. Lynch, R. R. Gamache, and S. P. Neshyba, J. Quant. Spectrosc. Radiat. Transf. **59**, 595 (1998).
[13] R. R. Gamache, R. Lynch, and S. P. Neshyba, J. Quant. Spectrosc. Radiat. Transf. **59**, 319 (1998).
[14] J. M. Hartmann, C. Camy-Peyret, J. B. J. M. Flaud, and D. Robert, J. Quant. Spectrosc. Radiat. Transf. **40**, 489 (1988).
[15] S. Bouazza, A. Barbe, J. J. Plateaux, L. Rosenmann, J. M. Hartmann, C. Camypeyret, J. M. Flaud, and R. R. Gamache, J. Mol. Spectrosc. **157**, 271 (1993).
[16] D. Priem, J.-M. Colmont, F. Rohart, G. Wlodarczak, and R. R. Gamache, J. Mol. Spectrosc. **204**, 204 (2000).
[17] B. J. Drouin, J. Fischer, and R. R. Gamache, J. Quant. Spectrosc. Radiat. Transf. **83**, 63 (2004).
[18] G. Blanquet, J. Walrand, and J.-P. Bouanich, J. Mol. Spectrosc. **201**, 56 (2000).
[19] J.-P. Bouanich, G. Blanquet, J. Walrand, and M. Lepere, J. Mol. Spectrosc. **218**, 22 (2003).
[20] G. Blanquet, J.-P. Bouanich, J. Walrand, and M. Lepere, J. Mol. Spectrosc. **222**, 284 (2003).
[21] J.-P. Bouanich, J. W. G. Blanquet, and M. Lepere, J. Mol. Spectrosc. **227**, 172 (2004).
[22] J.-P. B. G. Blanquet, J. Walrand, and M. Lepere, J. Mol. Spectrosc. **229**, 198 (2005).
[23] S. V. Ivanov, L. Nguyen, and J. Buldyreva, J. Mol. Spectrosc. **233**, 60 (2005).
[24] L. Nguyen, S. Ivanov, O. G. Buzykin, and J. Buldyreva, J. Mol. Spectrosc. **239**, 101 (2006).
[25] C. G. Gray and J. V. Kranendonk, Can. J. Phys. **44**, 2411 (1966).
[26] A. D. Bykov, N. N. Lavrentieva, and L. N. Sinitsa, Atmos. Oceanic Opt. **5**, 587 (1992).
[27] A. D. Bykov, N. N. Lavrentieva, and L. N. Sinitsa, Atmos. Oceanic Opt. **5**, 728 (1992).
[28] L. D. Landau and E. M. Lifchitz, *Course of Theoretical Physics* (Pergamon, Oxford, 1976), Vol. 1.
[29] J. Buldyreva, J. Bonamy, and D. Robert, J. Quant. Spectrosc. Radiat. Transf. **62**, 321 (1999).
[30] J. Buldyreva, S. Benec'h, and M. Chrysos, Phys. Rev. A **63**, 012708 (2000).
[31] P. Sinha, P. V. Hobbs, R. J. Yokelson, I. T. Bertschi, D. R. Blake, I. J. Simpson, S. Gao, T. W. Kirschstetter, and T. Novakov, J. Geophys. Res., [Atmos.] **108**, 8487 (2003).
[32] V. Kunde, A. C. Aiken, R. Hanel, D. E. Jennings, V. G. Kunde, and R. C. Samuelson, Nature (London) **292**, 686 (1981).
[33] T. Ancrenaz, M. Combes, Y. Zear, L. Vapillon, and J. Berezne, Astron. Astrophys. **42**, 355 (1975).
[34] T. Kostiuk, P. Romani, F. Espenak, T. A. Livengood, and J. J. Goldstein, J. Geophys. Res., [Planets] **98**, 18823 (1993).
[35] W. E. Blass *et al.*, J. Quant. Spectrosc. Radiat. Transf. **71**, 47 (2001).
[36] F. Thibault, B. Calil, J. Buldyreva, M. Chrysos, J.-M. Hartmann, and J.-P. Bouanich, Phys. Chem. Chem. Phys. **3**, 3924 (2001).
[37] M. E. Rose, *Elementary Theory of Angular Momentum* (Wiley, New York, 1957).
[38] R. P. Leavitt, J. Chem. Phys. **73**, 5432 (1980).
[39] C. G. Gray, Can. J. Phys. **46**, 135 (1968).
[40] C. G. Gray and K. E. Gubbins, *Theory of Molecular Fluids* (Clarendon, Oxford, 1984), Vol. 1.
[41] G. Herzberg, *Molecular Spectra and Molecular Structure. II. Infrared and Raman Spectra of Polyatomic Molecules* (Van Nostrand, Princeton, NJ, 1968).
[42] W. Gordy, W. V. Smith, and R. F. Trambarulo, *Microwave Spectroscopy* (Wiley, London, 1953).
[43] T. B. Macrury, W. A. Steele, and B. J. Berne, J. Chem. Phys. **64**, 1288 (1976).
[44] H. Yasuda and T. Yamamoto, Prog. Theor. Phys. **45**, 1458 (1971).
[45] J. Downs, K. E. Gubbins, S. Murad, and C. G. Gubbins, Mol. Phys. **37**, 129 (1979).
[46] D. A. Varshalovich, A. N. Moskalev, and V. K. Khersonskii, *Quantum Theory of Angular Momentum* (World Scientific, Singapore, 1988).
[47] J.-P. Bouanich, G. Blanquet, J. C. Populaire, and J. Walrand, J. Mol. Spectrosc. **190**, 7 (1998).
[48] M. Rotger, W. Raballand, V. Boudon, M. Loete, J. Breidung, and W. Thiel, *Stark Effect in X2Y4 Molecules: Application to Ethylene, XIXth International Conference on High Resolution Molecular Spectroscopy*, Salamanca, Spain (Universidad de Salamanca, Salamanca, 2005).